Ye et al. BMC Oral Health (2025) 25:840
https://doi.org/10.1186/s12903-025-06082-3

BMC Oral Health

RESEARCH Open Access

Cancer-associated fibroblasts-derived exosomal piR-35462 promotes the progression of oral squamous cell carcinoma via FTO/Twist1 pathway

Yushan Ye[1,2†], Fan Wu[1,2†], Bowen Li[1,2†], Hanyu Ma[3], Lianxi Mai[1,2], Yu Peng[4], Xiaodi Feng[1,2], Xiao Tan[1,2], Min Fu[1,2], Yongmei Tan[1,2], Tianjun Lan[1,2], Ruixin Wang[1,2], Siqi Ren[1,2], Jinsong Li[1,2*], Shaohai Chang[1,2*] and Shule Xie[1,2*]

Abstract

Background Cancer-associated fibroblasts (CAFs) represent a crucial component of tumor stroma and play critical roles in cancer progression. However, the role of CAFs derived exosomes in oral squamous cell carcinoma (OSCC) environment is unexplored. PIWI-interacting RNAs (piRNAs) serve as epigenetic effectors in cancer progression and constitute significant compositions of exosomes. Here, we explored the functional mechanism of exosomal piRNAs in OSCC development.

Methods We screened exosomal piRNAs derived from CAFs and normal fibroblasts (NFs) and assess their effect on tumor proliferation and metastasis. A nude mouse model was established to assess the impact of exosomal piR-35462 on tumor progression.

Results CAFs-derived exosomes showed an enhanced piR-35462 expression and promoted OSCC cell proliferation, migration and invasion. Additionally, elevated piR-35462 expression in OSCC tissues correlates with poor prognosis. Mechanistically, CAFs-derived exosomal piR-35462 increased the expression of fat mass and obesity-associated protein (FTO) in OSCC cells. By inhibiting N6-methyladenosine (m6A) RNA methylation, the overexpression of FTO further enhances the stability and expression levels of Twist1 mRNA, thereby contributing to epithelial-mesenchymal transition (EMT) and tumor progression. In vivo xenograft tumor model also confirmed the same results.

Conclusion The achieved outcomes elucidate that CAFs can deliver piR-35462 containing exosomes to OSCC cells and promote OSCC progression via FTO/Twist mediated EMT pathways, and could represent a promising therapeutic target for OSCC.

†Yushan Ye, Fan Wu and Bowen Li contributed equally to this work.

*Correspondence:
Jinsong Li
lijinsong1967@163.com
Shaohai Chang
changshh@mail.sysu.edu.cn
Shule Xie
xieshle3@mail.sysu.edu.cn

Full list of author information is available at the end of the article

Keywords Cancer-associated fibroblasts, Oral squamous cell carcinoma, Exosome, piRNA, Epithelial-mesenchymal transition

Introduction

OSCC, a prevalent global malignancy, exhibits a five-year survival rate of merely 50% [1–3]. Recent studies underscore the tumor microenvironment's essential role in initiating and advancing tumors [4–6], underscoring the necessity to decipher the molecular mechanisms influencing OSCC tumorigenesis and metastasis within its TME.

CAFs, a subtype of activated fibroblasts within the TME, are implicated in various aspects of cancer progression [7–10]. Predominant in the TME of both primary and metastatic tumors, CAFs significantly contribute to tumor growth, invasion, and metastasis [11–13]. However, the mechanisms underlying CAF functions remain partially understood. Concurrently, evidence is mounting on the pivotal role of exosomes from CAFs in TME intercellular communication [14–18], transferring critical biomolecules such as DNA, RNA, proteins, and lipids that influence tumor infiltration and distant metastasis. Among these molecules, PIWI-interacting RNAs (piRNAs), recently identified non-coding RNAs spanning 24 to 31 nucleotides, are known for their ability to regulate gene expression and maintain genomic integrity via PIWI protein targeting [19, 20]. Recent studies have identified abnormal piRNA expression in various cancers [21–28], yet the contribution of piRNAs from CAFs to OSCC invasion and metastasis is yet to be clarified.

The research presents the first evidence of piR-35462 being efficiently transferred from CAFs to OSCC cells via exosomes, promoting tumor proliferation, invasion, metastasis, and correlating with poor OSCC prognosis. Further mechanistic insights revealed that piR-35462 induces epithelial-mesenchymal transition in OSCC cells via modulating the stability of Twist1 mRNA. This research uncovers a novel regulatory pathway for OSCC invasion and metastasis, positioning piR-35462 as a potential oncogenic factor derived from CAFs. Our findings offer novel insights into the molecular underpinnings of OSCC invasion and metastasis, potentially paving the way for therapeutic interventions targeting piR-35462.

Materials and methods

Additional information is provided in the Supplementary Materials and Methods.

Approval of ethics

This research received approval from the Institutional Review Board at Sun Yat-Sen Memorial Hospital, China (No. SYSKY-2024-014-01).

Culture and transfection of cells

CAFs and NFs were extracted from OSCC patient surgical specimens. The OSCC cell lines SAS and CAL27 were procured from the American Type Culture Collection (ATCC, US). Transfections were conducted following the manufacturer's instructions [29].

Inhibitor, mimic, as well as plasmid construction

The cDNA encoding Fat Mass and Obesity-Associated Protein (FTO) was inserted into the pcDNA3.1-Myc/His vector (Invitrogen, US) and its sequence was confirmed. Wild type (WT) FTO 3'-UTR sequences were cloned into pmiRGLO vectors (Promega, US) for luciferase assays. Mutated (MUT) luciferase reporters were created employing PCR-based site-directed mutagenesis. piR-35462 mimics, inhibitors, FTO shRNA, and control sequences were produced by Shanghai GenePharma (China), as outlined in Table 1.

Exosome isolation as well as fluorescent labeling

Exosomes were extracted from conditioned media employing differential ultracentrifugation methods detailed in prior studies [30]. Characterization of exosomes was conducted via Nanoparticle Tracking Analysis with a ZetaView PMX 110 (Particle Metrix, Germany) and confirmed through transmission electron microscopy. Exosomes were fluorescently labeled employing the PKH26 kit, adhering to the manufacturer's protocol [31].

Fluorescence in situ hybridization and Immunofluorescence assay

For the FISH procedure, a commercial kit (RiboBio, China) was employed according to the manufacturer's guidelines [32]. Briefly, CAL27 and SAS cells were inoculated in a 24- well plate and fixed by 10% paraformaldehyde. After being treated with protease K, Cells in a glass-bottom dish overnight were incubated with prehybridization solution at 37℃ for 30 min. Then, hybridization solution containing 20 μM piR-35462 probes was added to slides and the cells were incubated at 42 °C overnight. Next day, cells were washed with saline sodium citrate (SSC) solution. The nuclei were incubated with DAPI for 10 min at room temperature. Finally, the results were examined employing a fluorescence microscope (LSM5, Carl Zeiss, Germany).

Protein assessment via Western blot

The Western blot experimental procedure was conducted in accordance with previously documented methods [33].

Table 1 The sequence of inhibitor, mimics and ShRNAs

Name	Sequence
piR-35462 inhibitor	UGAUGCUCUACCAACUGAGCUAUCCAGGC
piR-35462 mimics	GCCUGGAUAGCUCAGUUGGUAGAGCAUCA
piR-NC	UUCUCCGAACGUGUCACGUTT
FTO shRNA	GGATGACTCTCATCTCGAA
Rab27A shRNA	GCTGCCAATGGGACAAACATA

Table 2 Stem-loop reverse transcription primers

Genes	RT primer sequences
piR-33,082	GTCGTATCCAGTGCGTGTCGTGGAGTCG-GCAATTGCACTGGATACGACAATCTG
piR-33,160	GTCGTATCCAGTGCGTGTCGTGGAGTCG-GCAATTGCACTGGATACGACATCTGT
piR-60,565	GTCGTATCCAGTGCGTGTCGTGGAGTCG-GCAATTGCACTGGATACGACGCCGAA
piR-35,467	GTCGTATCCAGTGCGTGTCGTGGAGTCG-GCAATTGCACTGGATACGACCTGATG
piR-35,952	GTCGTATCCAGTGCGTGTCGTGGAGTCG-GCAATTGCACTGGATACGACGCTATG
piR-36,225	GTCGTATCCAGTGCGTGTCGTGGAGTCG-GCAATTGCACTGGATACGACAGCATGCGCT
piR-36,244	GTCGTATCCAGTGCGTGTCGTGGAGTCG-GCAATTGCACTGGATACGACAGCACGCGCT
piR-35462	GTCGTATCCAGTGCGTGTCGTGGAGTCG-GCAATTGCACTGGATACGACTGATGC
piR-56,450	GTCGTATCCAGTGCGTGTCGTGGAGTCG-GCAATTGCACTGGATACGACCCTCGATCAG
piR-41,525	GTCGTATCCAGTGCGTGTCGTGGAGTCG-GCAATTGCACTGGATACGACCCATTTTGTAGGTT
U6	TTCACGAATTTGCGTGTCAT′

Molecular characterization involved qPCR, RNA-seq, as well as Rna stability evaluation

Total RNA isolation was carried out employing TRIzol reagent (Invitrogen, US) following the manufacturer's instructions. Detailed information regarding the reverse transcription primers is provided in Table 2. Primer sequences for qPCR are outlined in Table 3. Gene Set Enrichment Analysis (GSEA) identified potential target genes. RNA stability assessments involved treating OSCC cells with actinomycin D (Santa Cruz, 5 μM), collecting samples at specified intervals for qPCR, and calculating mRNA stability (t1/2) in comparison to GAPDH.

Cell proliferation assessment

Proliferation assessment utilized the Cell Counting Kit-8 (CCK-8) and EdU cell proliferation assays, following manufacturer guidelines [34, 35]. Proliferation rates were monitored every 24 h with a multiscanner autoreader (BioTek, VT, US) and a fluorescence microscope (Nikon, Japan).

Assessment of cell migration as well as invasion

Migration and invasion assessments were carried out employing Transwell chambers as previously described [36, 37].

Assay of dual luciferase reporter

For the dual luciferase reporter assay, cells were co-transfected with plasmids harboring either the wild-type

Table 3 Primer sequences used for qPCR

Genes	Forward sequence	Reverse sequence
FAP	GGAAGTGCCTGTTCCAGCAATG	TGTCTGCCAGTCTTCCCTGAAG
α-SMA	AAAAGACAGCTACGTGGGTGA	GCCATGTTCTATCGGGTACTTC
Vimentin	GACGCCATCAACACCGAGTT	CTTTGTCGTTGGTTAGCTGGT
GAPDH	GGAGCGAGATCCCTCCAAAAT	GGCTGTTGTCATACTTCTCATGG
METTL14	AGTGCCGACAGCATTGGTG	GGAGCAGAGGTATCATAGGAAGC
Twist1	GGCTCAGCTACGCCTTCTC	TCCATTTTCTCCTTCTCTGGAA
ALKBH5	AGTTCCAGTTCAAGCCTATTCG	TGAGCACAGTCACGCTTCC
METTL3	TTGTCTCCAACCTTCCGTAGT	CCAGATCAGAGAGGTGGTGTAG
FTO	ACTTGGCTCCCTTATCTGACC	TGTGCAGTGTGAGAAAGGCTT
Rab27A	ATGTCTGATGAGGATTATGATTACCTC	GAGTTCAGAGGGAAGATACGAGCCAAGAGA
piR-35462	GCCTGGATAGCTCAGTTGGTAGA	CAGTGCGTGTCGTGGAGT
piR-33,082	CCGGACACGGACAGGATTGA	CAGTGCGTGTCGTGGAGT
piR-33,160	CCCGGACACGGACAGGATT	CAGTGCGTGTCGTGGAGT
piR-60,565	TTCCCTGGTGGTCTAGTGGTTAGGA	CAGTGCGTGTCGTGGAGT
piR-35,467	GCCTGGGTAGCTCAGTCGGTAGAG	CAGTGCGTGTCGTGGAGT
piR-35,952	AGCGTTGGTGGTATAGTGGTGAG	CAGTGCGTGTCGTGGAGT
piR-36,225	GGGGATGTAGCTCAGTGGTAGAG	CAGTGCGTGTCGTGGAGT
piR-36,244	GGGGGTNTAGCTCAGTGGTAG	CAGTGCGTGTCGTGGAGT
piR-35462	GCCTGGATAGCTCAGTTGGTAGA	CAGTGCGTGTCGTGGAGT
piR-56,450	GGGCCCAAGTCCTTCTGA	CAGTGCGTGTCGTGGAGT
piR-41,525	TCGCCGTGTTAAATAGCAAAG	CAGTGCGTGTCGTGGAGT
U6	CGCTTCGGCAGCACATATAC′	TTCACGAATTTGCGTGTCAT

(WT) or mutant (MUT) FTO 3′-UTR sequences in conjunction with piRNA inhibitors employing Lipofectamine 3000 (Invitrogen, US). Forty-eight hours post-transfection, firefly and Renilla luciferase activities were quantified employing the Dual-Luciferase Reporter Assay System (Promega, US), in adherence to the manufacturer's protocol [38].

Tumorigenesis and metastasis in vivo

Twenty female BALB/c nu/nu mice, were procured from the Guangdong Medical Laboratory Animal Center (SCXK [Yue] 2013-0002). A lateral dorsal subcutaneous injection was administered. Tumor growth was monitored weekly employing Vernier calipers. Mice were euthanized by CO_2 inhalation until respiratory and cardiac arrest. All procedures were conducted in compliance with the Institutional Animal Care and Use Committee's sanctioned protocols (SYSU-IACUC-2024B10019).

Determination of m6A level

For m6A level determination, mRNA was isolated with the Dynabeads mRNA Purification Kit (Thermo Scientific). The global m6A methylation status of the purified mRNA was assessed employing the EpiQuik m6A RNA Methylation Quantification Kit (Epigentek, Germany), following the instructions provided. The assay utilized 200 ng of poly-A-enriched RNA.

Statistical assessment

Statistical analysis was performed employing GraphPad Prism 9.0 (GraphPad Software, US) and SPSS 22.0 (IBM, US). Significance levels set at $^{*}p < 0.05$, $^{**}p < 0.01$, and $^{***}p < 0.001$.

Results

CAFs-Derived exosomes enhance OSCC cell proliferation, migration, as well as invasion

CAFs as well as NFs were isolated from oral squamous cell carcinoma and surrounding non-tumor tissues, respectively. They exhibited a spindle shape and were confirmed as fibroblasts through positive immunofluorescence staining for fibroblast-specific markers (Fig. 1A). Compared to NFs, CAFs showed elevated levels of α-smooth muscle actin (α-SMA) and fibroblast activation protein (FAP) (Fig. 1A-C). Exosomes, pivotal for cellular communication within the tumor microenvironment, were isolated from CAFs and NFs-conditioned mediums (CM) via ultracentrifugation [39]. Their presence was validated by western blotting and electron microscopy, revealing an average diameter of 219 nm (range 30–220 nm) and characteristic double-layered membranes (Fig. 1D, F). Elevated levels of exosomal markers CD63 and TSG101 and the absence of calnexin, an endoplasmic reticulum marker, were noted in fibroblast-derived exosomes (Fig. 1E). The incorporation of exosomes derived from fibroblasts into OSCC cells was demonstrated through PKH26 fluorescent dye labeling; red fluorescence observed in SAS and CAL27 cells after three hours of co-culture indicated successful absorption of these exosomes by OSCC cells (Fig. 1G).

An investigation into the effects of CAFs-secreted exosomes on OSCC cell proliferation, invasion, and migration was conducted. Experiments with SAS and CAL27 cell lines demonstrated that CAFs-derived exosomes significantly augmented cell proliferation compared to exosomes from NFs, as shown by CCK8 and EdU assays (Fig. 2A, B). Furthermore, the presence of CAFs-derived exosomes considerably elevated the migratory and invasive capabilities of both SAS and CAL27 cells (Fig. 2C). Treatment with CAFs-secreted exosomes resulted in the upregulation of mesenchymal markers Twist1 and Vimentin and a decrease in the epithelial marker E-cadherin in both cell lines (Fig. 2D).

To further delineate the contributions of exosomes to OSCC cell dynamics, particularly focemploying on growth, migration, as well as invasion, supernatants devoid of exosomes were obtained through ultracentrifugation. It was determined that CAFs facilitated oral cancer cell proliferation and migration via exosomes rather than via co-purifying complexes found in ultracentrifuged pellets (Fig. S1A, B), indicating a pivotal role of CAFs-secreted exosomes in OSCC cell dynamics.

piR-35462 enrichment in CAFs-Derived exosomes correlates with OSCC patient survival

Exosomes are known to be rich in small non-coding RNAs, crucial for intercellular communication [40]. Through small RNA-sequencing of exosomes extracted from three pairs of CAFs and NFs, numerous small RNAs, particularly piRNAs, exhibited differential expression (adjusted p-value less than 0.05 and fold change more than 2) between the two groups (Fig. 3A). Further analysis of the highest ranked ten piRNAs from 20 pairs of NFs or CAFs-derived exosomes revealed a significant increase in piR-35462 and piR-60,565 levels in CAFs-derived exosomes (Fig. 3B). Additionally, the assessment of piRNA expressions was carried out in 76 matched pairs of OSCC and adjacent normal tissues. qPCR analysis showed elevated levels of piR-35462, but not piR-60,565, in OSCC tissues (Fig. 3C, S2A). Elevated piR-35462 expression was also significant in both recipient OSCC cells and CAFs (Fig. 3D, E, and S2B, C). piR-35462 expression was notably associated with the N stage, with no significant correlation to age, gender, T stage, or pathological stage (Table 4). High levels of piR-35462 were indicative of reduced overall survival in OSCC patients (Fig. 3E), suggesting a potential oncogenic role of piR-35462 in OSCC progression.

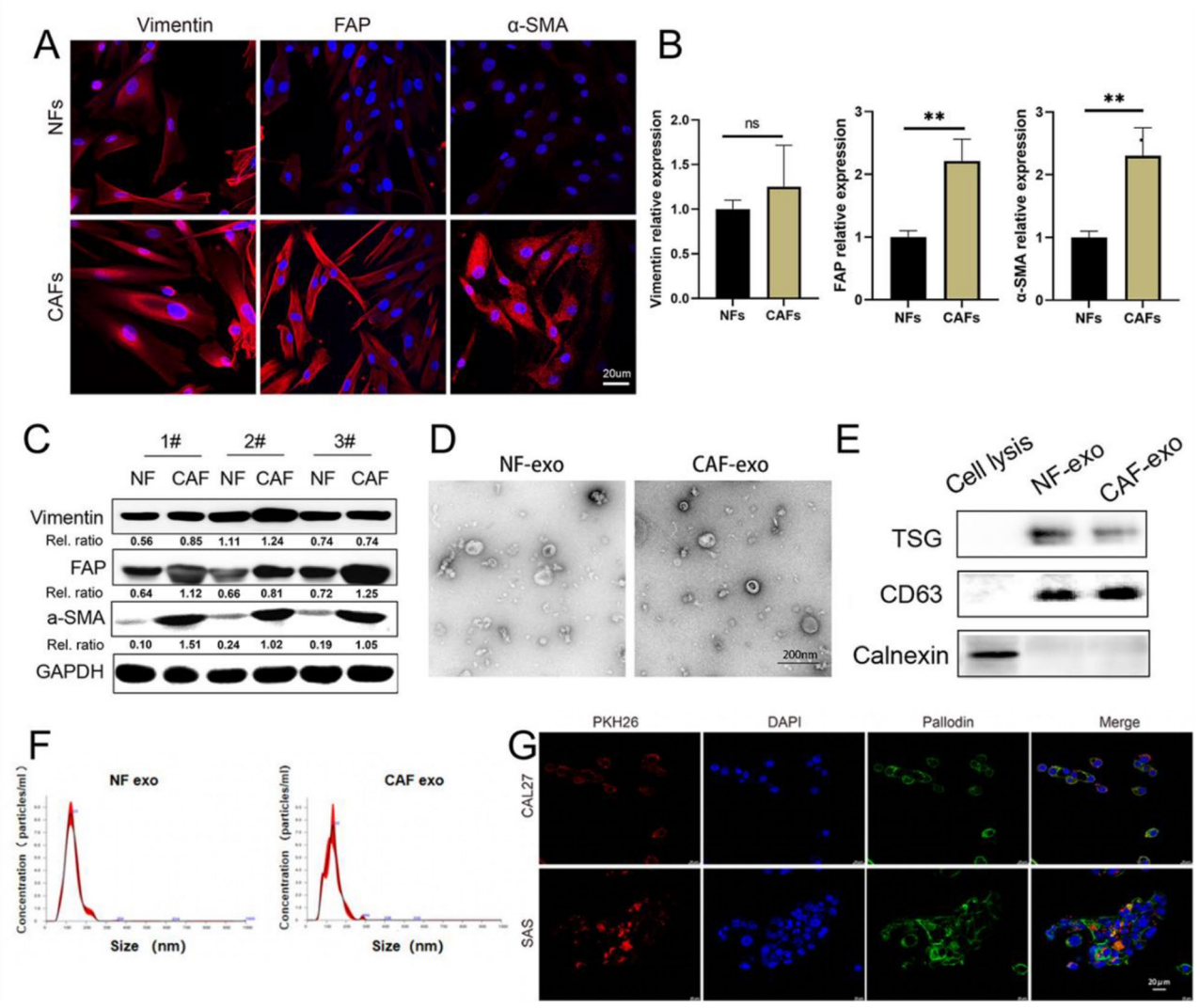

Fig. 1 Characteristics of CAFs derived from OSCC patients and isolation of exosomes. (**A**) Immunofluorescent staining and quantification of α-SMA, FAP and vimentin expression in NFs and CAFs (scale bar, 20 μm). (**B**)qPCR and (**C**)western blotanalysis of α-SMA, FAP and vimentin protein levels in three pairs of NFs and CAFs. (**D**)Electron microscopy analysis of exosomes isolated from NF- or CAFs-conditioned medium (scale bar, 200 nm). (**E**)Western blot analysis of CD63, HSP70, calnexin and GM130 expression in exosomes isolated from NFs, CAFs and in cell lysates. (**F**)Nanoparticle tracking analysis of vesicles collected from NF- or CAFs-conditioned medium. (**G**) Representative microscopy image showing the uptake of PKH26-labeled exosomes by SAS and CAL27 cells. Three independent experiments were performed and representative images are shown (scale bar, 20 μm). Data are presented as means ± SEM (*$p < 0.05$; **$P < 0.01$; ***$P < 0.001$)

To ascertain if the elevation of piR-35462 in OSCC cells resulted from transfer via CAFs-derived exosomes, actinomycin D was introduced into the co-culture system. This intervention did not alter piR-35462 levels in OSCC cells, negating the theory of an endogenous source for the increase (Figure S2D). Reduction of exosome secretion was achieved through treatment with GW4869 (an nSMase inhibitor) or knockdown of Rab27a via shRNAs, which predictably decreased piR-35462 and piR-60,565 levels in CM from CAFs (Fig. 3G, S2E). RNA fluorescence in FISH analysis disclosed the presence of piR-35462 within both the nucleus and cytoplasm of OSCC cells following exosome uptake (Fig. 3H). Collectively, these findings demonstrate that piR-35462 is upregulated in exosomes from CAFs and in OSCC tissues, correlating with an adverse prognosis for OSCC patients.

Augmentation of Exosomal piR-35462 in CAFs enhances oral Cancer progression

The impact of CAFs-released exosomal piR-35462 on OSCC advancement was further investigated. To assess the capability of CAFs to transfer exosomal piR-35462 to OSCC cells, exosomes from CAFs, either transfected with piR-35462 mimics or a control, were introduced to SAS and CAL27 cell cultures. Notably, after 24 h of exposure to exosomes from CAFs genetically modified

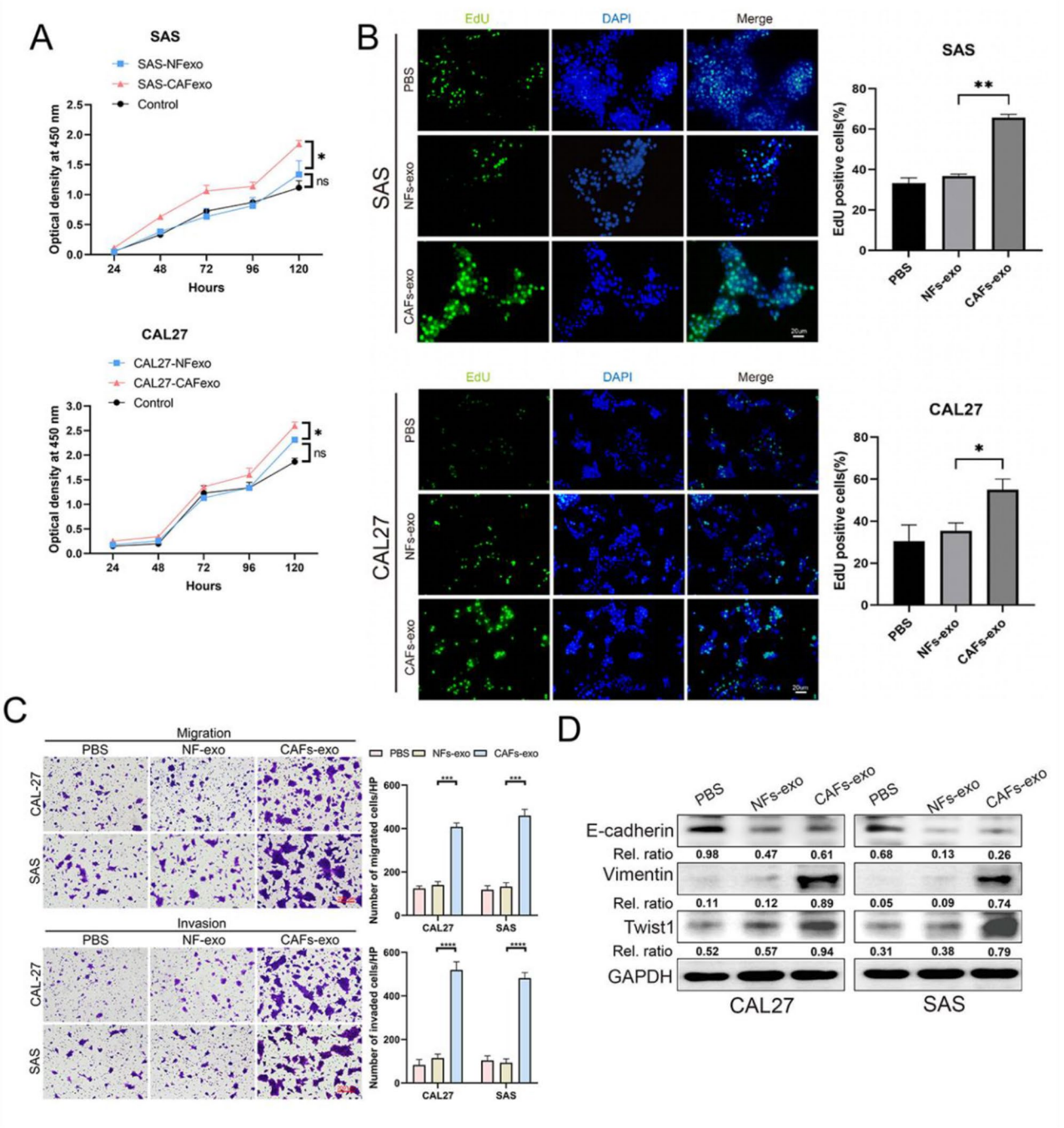

Fig. 2 CAF promotes the proliferation and migration of breast cancer cell through exosomes. (**A**, **B**) The relative proliferation ability was analyzed in CCK-8 and EdU assays of SAS and CAL27 cells after incubation with NFs- or CAFs-derived exosomes (scale bar, 20 μm). (**C**) SAS and CAL27 cells were incubated with NFs- or CAFs-derived exosomes or co-cultured with NFs or CAFs using Boyden chambers. Transwell assays were performed to detect the cell migration and invasion (scale bar, 20 μm). Three independent experiments were performed and data are presented as means ± SEM (*$P < 0.05$; **$P < 0.01$; ***$P < 0.001$)

to express Cy3-tagged piR-35462 mimics, both CAL27 and SAS cells displayed red fluorescence (Fig. S3A). Subsequent qRT-PCR analysis post-24-hour exosome exposure revealed a significant increase in piR-35462 within the recipient cells (Fig. 4A). The addition of exosomes from CAFs overexpressing piR-35462 to the OSCC cell culture media led to a marked enhancement in cell proliferation, as evidenced by CCK-8 and EdU assays (Fig. 4B, C and S3B). Furthermore, exosomal piR-35462 positively influenced OSCC cell migration and invasion under co-culture conditions (Fig. 4D). These findings validate the

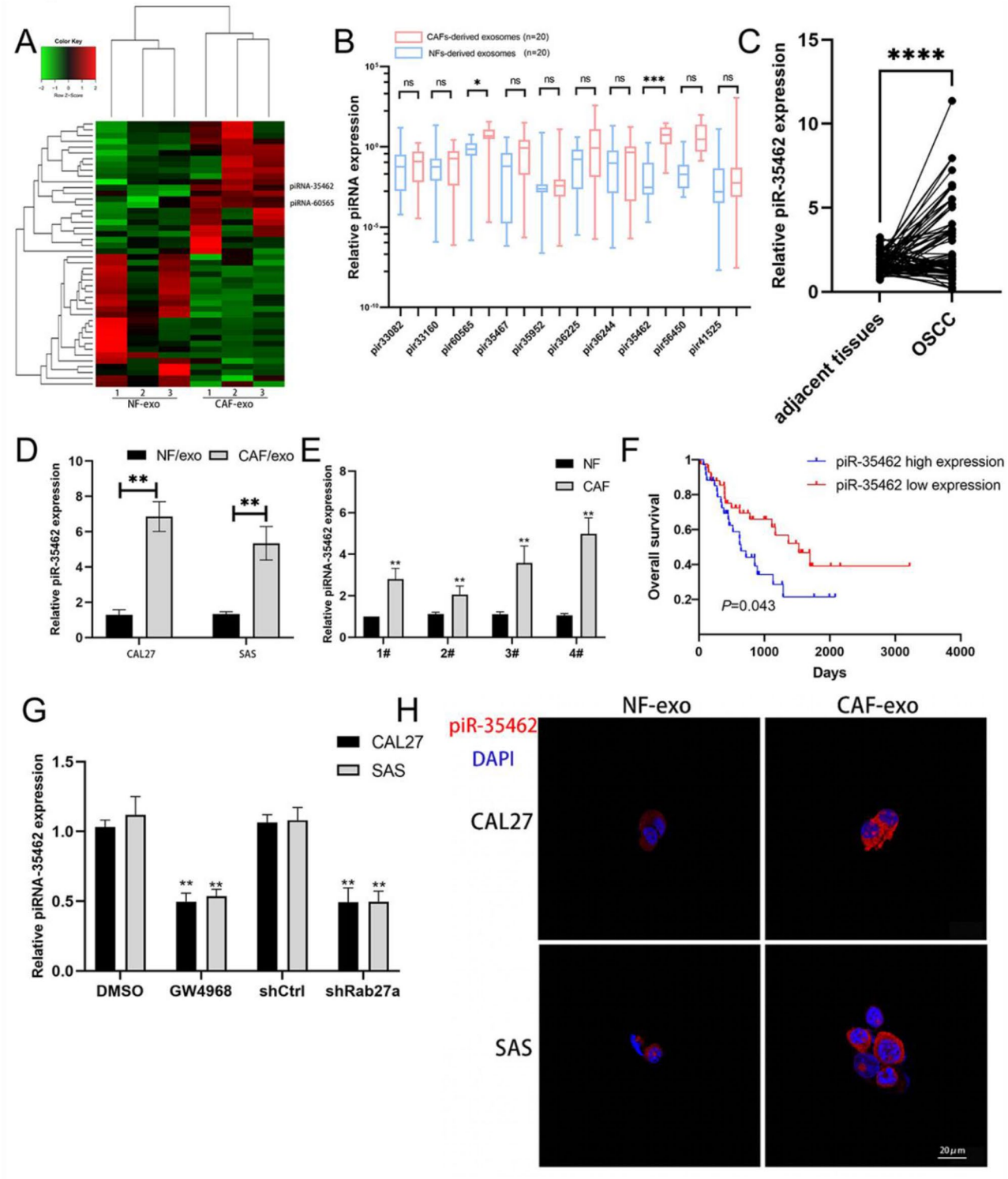

Fig. 3 piR-35462 is upregulated in CAFs-derived exosomes. (**A**) The heat map shows the expression of dysregulated piRNAs in exosomes derived from three pairs of CAFs or NFs. (**B**) The expression of top 10 piRNAs was examined in exosomes derived from 20 pairs of CAFs or NFs. (**C**) qPCR showing the expression of piR-35462 in OSCC and adjacent normal tissues. (**D**) qPCR showing the expression of piR-35462 in recipient cells treated with CAFs- or NFs-derived exosomes. (**E**) qPCR showing the expression of piR-35462 in four pairs of CAFs and NFs. (**F**) Kaplan-Meier analysis indicating the relationship between piR-35462 expression and overall survival in OSCC patients ($n = 76$, $P = 0.043$). (**G**) After co-cultivation with CAFs-derived exosomes treated with GW4869 (20μM) or shRab27a, piR-35462 expression was detected in the recipient cells. (**H**) Fluorescence in situ hybridization (FISH) of piR-35462 in recipient OSCC cells (scale bar, 20 μm). Data are presented as means ± SEM (*$P < 0.05$; **$P < 0.01$; ***$P < 0.001$)

Table 4 Baseline data table of 76 patients

	Constitute(%)		
Category	**piR-35462 high expression (*n* = 38)**	**piR-35462 low expression (*n* = 38)**	***P* value**
Age	45.3 (32–81)	51.4 (30–86)	0.562
Gender			
Male	20 (52.63)	25 (65.22)	
Female	18 (47.37)	13 (34.21)	0.243
Smoking or not			
Non-smoking	17 (44.74)	20 (52.63)	
Smoking	21 (55.26)	18 (47.37)	0.491
N stage[a]			
N0	13 (34.21)	26 (69.57)	
N1 + N2	25 (65.79)	12 (31.58)	0.003
Stages[a]			
I	13 (34.21)	15 (39.47)	
II	8 (21.05)	10 (26.32)	
III	10 (26.32)	7 (18.42)	
IV	7 (18.42)	6 (15.79)	0.808

[a]American Joint Committeeon Cancer,7th Edition staging

ability of OSCC cells to internalize exosomes laden with piR-35462 mimics, promoting OSCC progression.

Subsequent experiments involved transfecting CAL27 and SAS cells with piR-35462 mimics or antagomir-35,462 to investigate the influence of piR-35462 on OSCC growth and metastatic capabilities (Fig. S3C). Proliferation assays, including CCK-8 and EdU, revealed that piR-35462 significantly accelerated cellular proliferation in CAL27 and SAS cells compared to controls, an effect that was counteracted by antagomir-35,462 (Fig. 5A-C, S3D). Moreover, enhanced cell migration and invasion were observed following piR-35462 overexpression, whereas its suppression notably curtailed OSCC cell metastasis (Fig. 5D). Given the pivotal role of EMT in cancer metastasis, we assessed the impact of altering piR-35462 levels on EMT marker expression. Western blot results indicated that elevating piR-35462 levels resulted in upregulation of mesenchymal markers and downregulation of epithelial markers (Fig. S3E). Collectively, these findings underscore the potent role of piR-35462 in fostering OSCC cell proliferation, invasion, and migration.

Exosomal piR-35462 from CAFs facilitates epithelial-mesenchymal transition (EMT) in OSCC cells through the FTO/Twist1 signaling pathway

To explore the influence of piR-35462, carried by exosomes from CAFs, on the behavior of OSCC cells, sequencing of RNA was conducted on CAL27 cells treated with exosomes from CAFs and NFs. This analysis identified distinct gene expression profiles between the groups, with a notable upregulation of genes associated with EMT in cells treated with CAFs-derived exosomes, particularly highlighting Twist1 as significantly elevated (Fig. 6A-C). This led to the hypothesis that piR-35462 from CAFs-derived exosomes might facilitate metastasis via Twist1-mediated EMT processes. Subsequent investigations confirmed that CAFs-derived exosomes carrying piR-35462 indeed augmented the expression of Twist1 as well as Vimentin within OSCC cells, a process mitigated by inhibiting piR-35462 (Fig. 6D). Given piRNA's lack of complete complementarity to its mRNA targets, further analysis revealed no direct binding sites between piR-35462 and Twist1 mRNA, suggesting an indirect regulatory mechanism.

The literature suggests piRNAs influence m6A methylation, prompting an examination of m6A levels post-piR-35462 inhibition [21, 24, 41], revealing a reduction in m6A methylation in OSCC cells (Fig. S3F). Analysis of m6A regulatory proteins, which could potentially interact with piR-35462, showed decreased FTO expression following piR-35462 inhibition (Fig. 6E). Notably, a potential interaction site between piR-35462 and the 3'UTR of FTO mRNA was identified, indicating that piR-35462 may indirectly modulate Twist1 expression via FTO and m6A methylation adjustments (Fig. 6F). Dual luciferase reporter assays further verified this regulatory pathway, showing reduced luciferase activity in cells with piR-35462 inhibition, an effect reversible by mutating the predicted binding site (Fig. 6G). Additionally, piR-35462 overexpression was found to stabilize FTO mRNA, as evidenced by actinomycin D assays (Fig. 6H), and Western blot analysis confirmed that CAFs-derived exosomes upregulated FTO expression, an effect nullified by piR-35462 depletion (Fig. 6D). Furthermore, downregulating FTO via shRNAs counteracted the EMT gene expression changes induced by CAFs-derived exosomes (Fig. S3G), with a positive correlation between FTO and Twist1 expressions observed within the TCGA database (Fig. S3H). Collectively, these findings suggest that exosomal piR-35462 from CAFs promotes OSCC cell EMT through the FTO/Twist1 signaling pathway, presenting a novel mechanism of OSCC progression and a potential target for therapeutic intervention.

piR-35462-containing exosomes derived from CAFs promote OSCC progression in a xenograft animal model

In an in vivo study, we validated the impact of CAFs-derived exosomal piR-35462 on OSCC progression by administering a lateral dorsal subcutaneous injection of a SAS cell mixture with either NFs, CAFs, or CAFs with shRab27a knockdown into nude mice. Tumors co-injected with CAFs exhibited significantly accelerated growth compared to those injected with NFs. Conversely, tumors from the CAFs-shRab27a group demonstrated reduced growth rates (Figs. 7A–C). Further analysis via qPCR revealed elevated levels of piR-35462 and Twist1 in

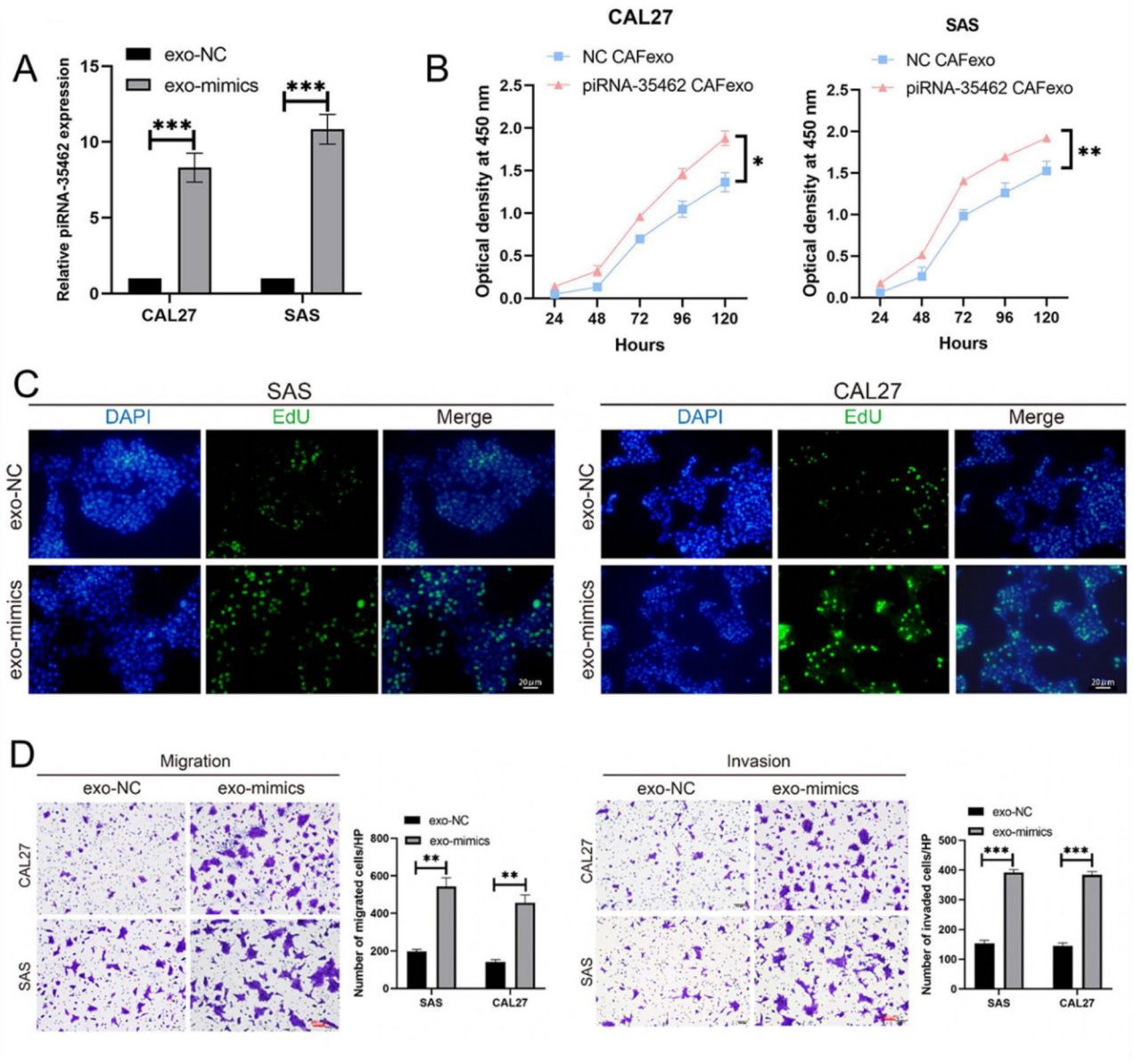

Fig. 4 piR-35462 upregulation in CAFs promotes cancer cell progression. (**A**) qPCR analysis of piR-35462 expression in recipient cells treated with CAFs-exo. (**B**,**C**) Cell proliferation was examined in recipient cells treated with CAFs-exo via CCK-8 and EdU assays (scale bar, 20 μm). (**D**) Transwell assays were utilized to assess the ability of cell migration and invasion in recipient cells (scale bar, 200 μm). Three independent experiments were performed and data are presented as means ± SEM (*$P < 0.05$; **$P < 0.01$; ***$P < 0.001$)

tumors co-cultured with CAFs compared to those with CAFs-shRab27a (Fig. 7D, E). Moreover, tumors from SAS cells mixed with CAFs showed decreased E-cadherin expression and increased Vimentin and Twist1 levels, indicative of enhanced EMT, a trend reversed in the CAFs-shRab27a group (Fig. 7F). These findings underscore the function of CAFs-derived exosomal piR-35462 in promoting OSCC tumor growth and metastasis by facilitating EMT in a xenograft mouse model.

Discussion

The challenge of managing local or regional recurrences and cervical lymph node metastases significantly complicates the clinical treatment of OSCC, impacting patient quality of life detrimentally [42]. The enhanced proliferative and migratory capabilities of OSCC cells contribute to treatment resistance and adverse patient prognoses. The underlying mechanisms driving OSCC metastasis and recurrence remain to be fully elucidated.

Recent findings highlight the tumor microenvironment (TME) as a critical facilitator of tumor invasion and

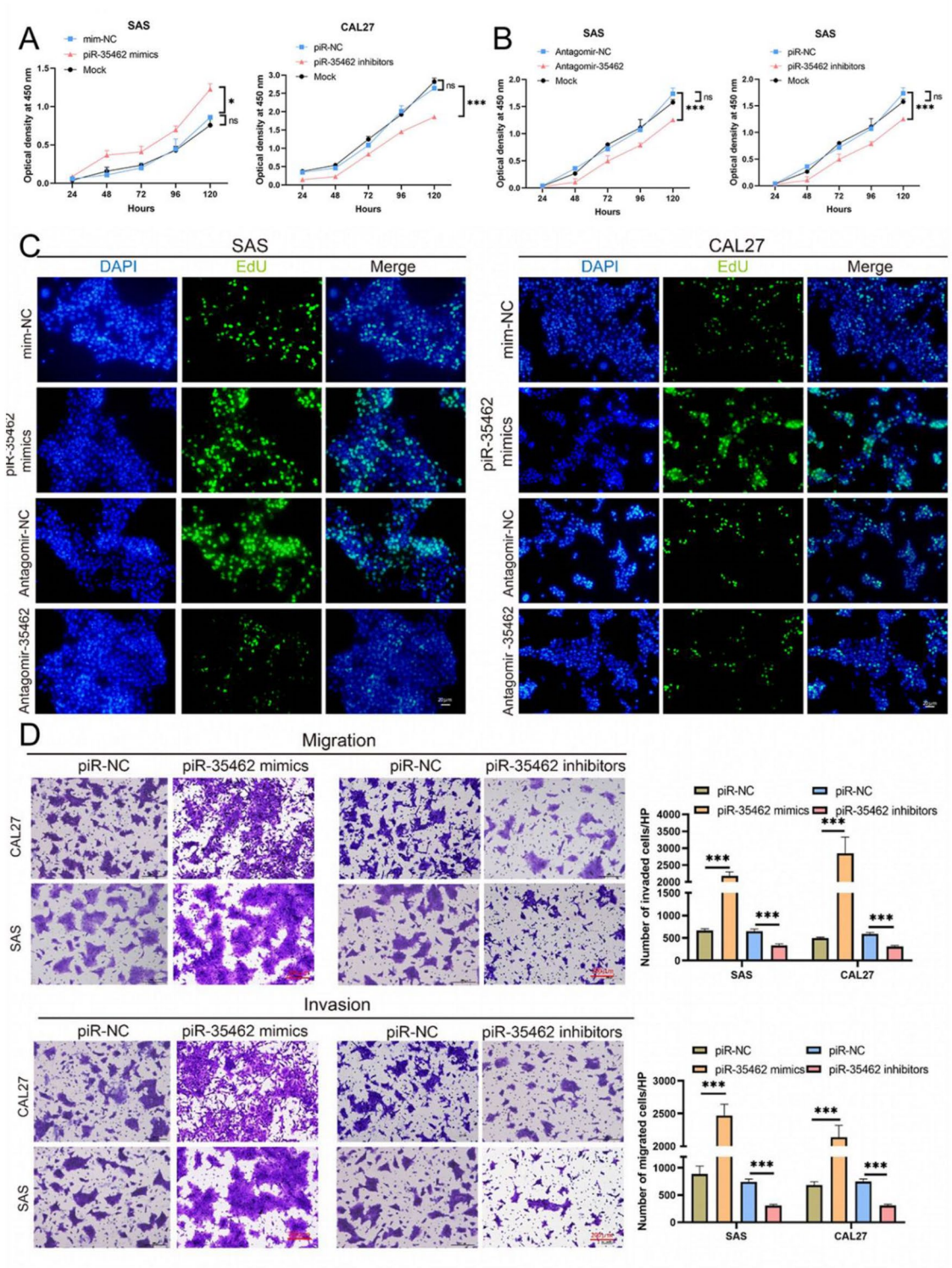

Fig. 5 piR-35462 promotes proliferation and metastasis of OSCC cells. (**A**-**C**) Cell proliferation (scale bar, 20 μm) and (**D**) migratory and invasive abilities were evaluated by CCK-8, EdU and Transwell assays, respectively in OSCC cells transfected with piR-35462 mimics, piR-35462 inhibitors or piR-NC (scale bar, 200 μm). Data are presented as means ± SEM (*$P < 0.05$; **$P < 0.01$; ***$P < 0.001$)

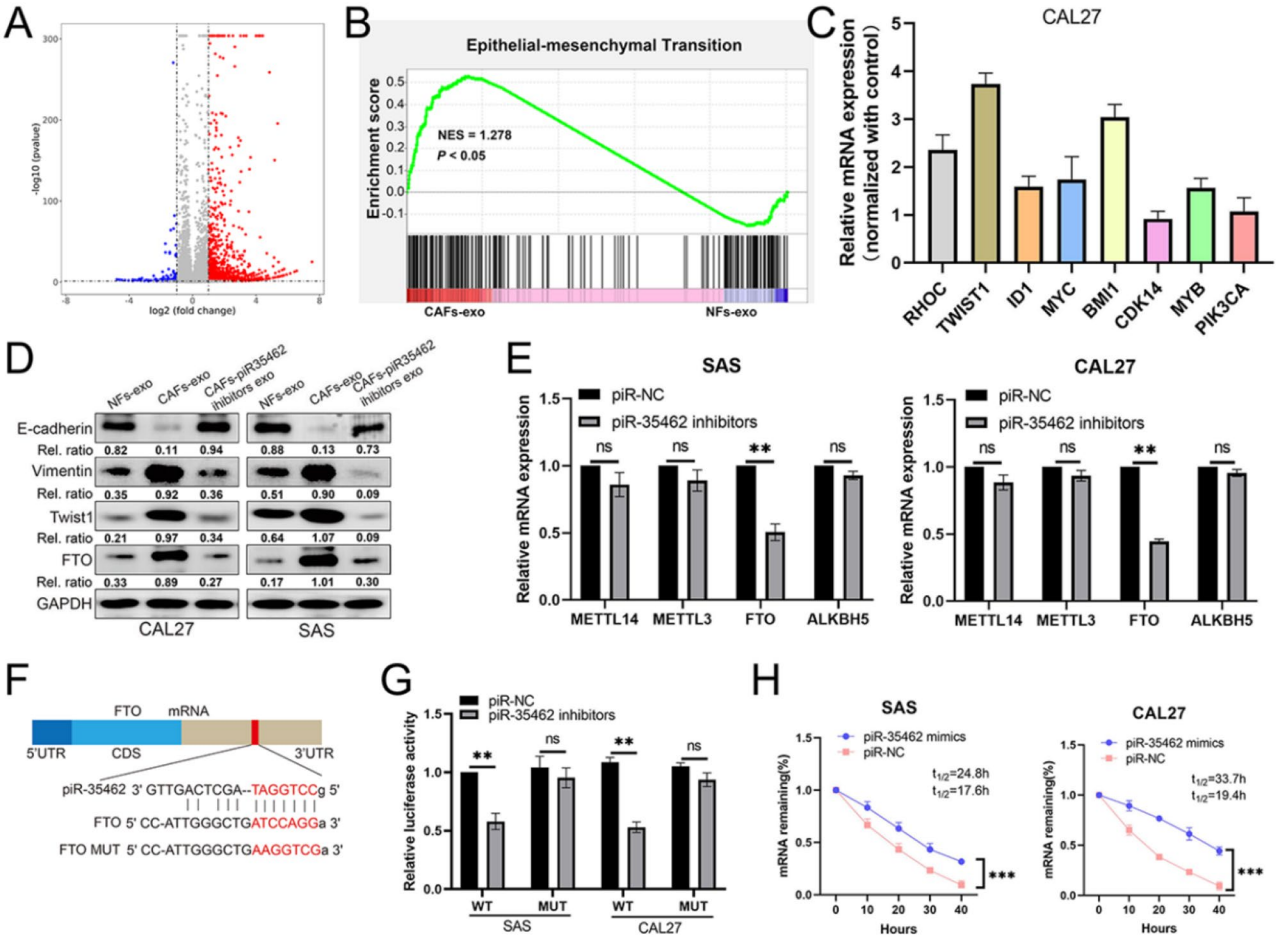

Fig. 6 Exosomal piR-35462 from CAFs promote the metastasis and EMT of OSCC cells via FTO/Twist1 signaling. (**A**) Volcano Plot showing the gene expression of CAL27 cells cultured with CAFs- or NFs-derived exosomes, examined by RNA sequencing. (**B**) Gene set enrichment analysis showing an enrichment of genes related to EMT in tumor cells cultured with CAFs-exo. Normalized enrichment score (NES) and false discovery rate (FDR) are indicated. (**C**) qPCR showing the expression of EMT related genes in CAL27 cells treated with CAFs-derived exosomes. (**D**) Western blot of E-cadherin, Vimentin, Twist1, and FTO in OSCC cells incubated with indicated exosomes. (**E**) qPCR was performed to detect METTL3, METTL14, ALKBH5 and FTO mRNA levels in SAS and CAL27 cells. (**F**) Diagram of the interaction between piR-35462 and the 3'UTR of FTO. (**G**) Luciferase reporter assays showing the effect of piR-35462 inhibitors on FTO reporters with either wild-type (WT) or mutated binding sites. (**H**) SAS and CAL27 cells were transiently transfected with piR-35462 mimics or piR-NC. The half-life (t1/2) of FTO mRNA was tested. Data represent the mean ± SD of at least three independent experiments. (*$P < 0.05$, **$P < 0.01$, ***$P < 0.001$)

metastasis, with CAFs playing a pivotal role in modulating these processes [43, 44]. As the predominant cell type within the TME, CAFs alter the TME landscape by secreting a diverse array of extracellular matrix proteins, cytokines, angiogenic factors, metabolites, and exosomes. This activity not only remodels local tissue architecture but also fosters tumor cell invasion and metastasis [17, 45, 46]. Given exosomes' role in mediating intercellular communication by transferring ncRNAs, proteins, and other molecules, it was postulated that CAFs-derived exosomes might endow tumor cells with enhanced proliferative and migratory abilities [47]. Compared to exosomes from NFs, a higher expression of various miRNAs lncRNA and circRNAs has been noted in CAFs-derived exosomes across different tumor types [48–50]. The question remains, however, whether CAFs-derived exosomes contain other components that could further encourage tumor proliferation and metastasis. In this study, we identified a novel piRNA, piR-35462, within CAFs-derived exosomes, revealing its potential to trigger EMT in OSCC.

In this investigation, we distinguished several piRNAs exhibiting substantial variance in CAFs-derived exosomes via non-coding RNA sequencing, noting that their abundance was marginally less than that of miRNAs. Specifically, piR-35462 was found to be markedly elevated in CAFs-derived exosomes, OSCC specimens, and among patients exhibiting adverse survival outcomes, as confirmed through in situ hybridization and qRT-PCR analyses. Additionally, our findings revealed that OSCC cells

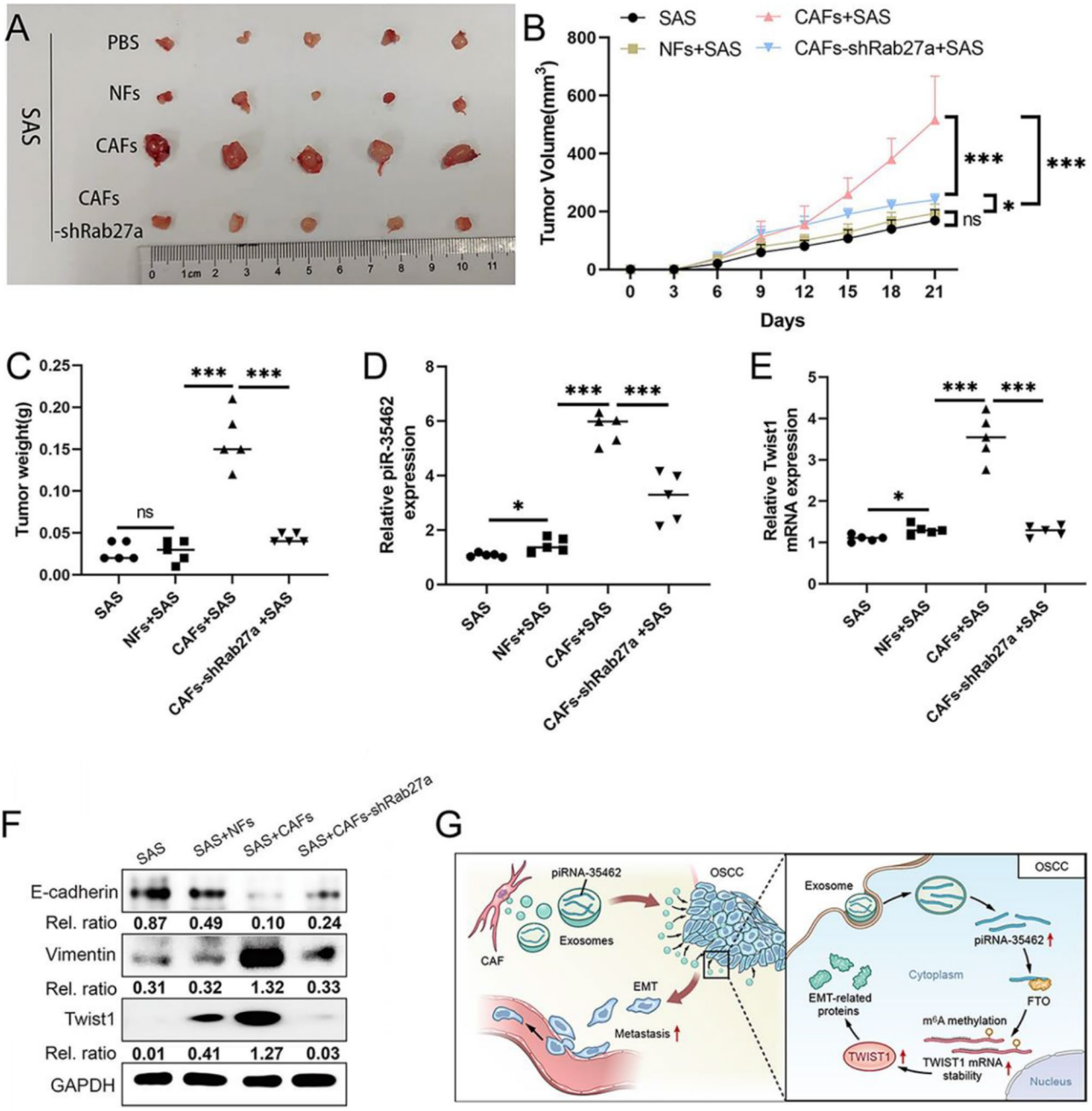

Fig. 7 piR-35462-containing exosomes derived from CAFs regulate the EMT pathway in vivo to promote OSCC tumour growth and metastasis. Nude mice were subcutaneously implanted with CAL27 cells treated using PBS, NFs, CAFs or CAFs-shRab27a. (**A**) Images of representative xenograft tumours. (**B**) Tumour volumes were analysed once weekly beginning 1 week after implantation. (**C**) Tumour weight were analysed after sacrifice. (**D**,**E**) The expression of piR-35462 and Twist1 was assessed via qPCR in tumours from different group. (**F**) E-cad, vimentin and Twist1 were analysed via Western blotting in tumour-bearing mice. (**G**) Schematic representation of the proposed mechanism. Data represent the mean ± SD of at least three independent experiments. (*$P < 0.05$, **$P < 0.01$, ***$P < 0.001$)

could internalize exosomes from CAFs, thereby acquiring piR-35462. Functionally, elevated piR-35462 levels were linked to increased OSCC cell proliferation, migration, and invasion, as demonstrated through CCK8, EDU, and Transwell assays conducted in vitro. Our in vivo investigations further elucidated piR-35462's role in facilitating popliteal lymph node metastasis in nude mice employing footpad xenografts. On a mechanistic level, the escalation of piR-35462 expression was observed to potentiate OSCC epithelial-mesenchymal transition via the FTO/Twist1 signaling pathway. Consequently, these findings underscore piR-35462's oncogenic role, highlighting its potential as a pivotal therapeutic target and diagnostic marker for OSCC.

Recent research into piRNA dysregulation across various cancers has highlighted its influential role in facilitating tumor cell growth, proliferation, metastasis, and progression [21–23]. Compared to other non-coding RNAs, piRNAs exhibit superior specificity, deliverability, and tolerability within tumors, which makes them the optimal targets for cancer therapy [51, 52]. PiRNAs, with their profound impact on epigenetic regulation, are emerging as pivotal diagnostic markers and therapeutic avenues across a spectrum of malignancies. For instance, in diffuse large B-cell lymphoma, the upregulation of piR-30,473 is associated with an aggressive cancer phenotype; its suppression, conversely, halts cell proliferation and triggers cell cycle arrest [24]. Another investigation has shown an increase in piR-DQ593109 within glomerular endothelial cells, assembling a piRNA-induced silencing complex with the PIWIL1 protein. This complex targets the long non-coding RNA MEG3 for degradation, leading to the suppression of ZO-1, occludin, and claudin-5 expression [53]. Furthermore, piRNAs have been identified as regulators of DNA methyltransferases, notably in breast cancer research, where piR-823 promotes DNA methylation of the adenomatous polyposis coli (APC) gene, thus activating the Wnt signaling pathway and fostering stemness in luminal breast cancer cells [25]. Our research highlights the critical role of piR-35462 in the post-transcriptional modulation of Twist1 through FTO-dependent m6A RNA demethylation, aligning with findings that piR-17,560 augments EMT and chemoresistance in breast cancer through similar mechanisms [41].

Conclusively, this study has established that CAFs-derived exosomes, rich in piR-35462, are instrumental in the transmission of this piRNA to OSCC cells, where it engages in FTO-mediated m6A demethylation to adjust the post-transcriptional activity of Twist1. This interaction precipitates EMT, thus promoting OSCC cell proliferation, invasion, as well as migration. These insights suggest piR-35462's potential as a promising candidate for therapeutic intervention and as a prognostic marker in OSCC management, offering new avenues for treatment strategies.

Conclusion

Our study unveiled the enrichment of an previously unreported piR-35462 in CAFs-derived exosomes. Subsequently, analysis revealed a correlation between elevated piR-35462 levels in OSCC tissues and an unfavorable prognosis. Furthermore, CAFs-derived exosomal piR-35462 was found to promote OSCC progression by inducing EMT. Mechanistically, we identified that piR-35462 promotes the progression of OSCC through the FTO/Twist1 pathway. These findings illuminate the role of CAFs in delivering piR-35462-containing exosomes to OSCC cells, thereby promoting OSCC progression through FTO/Twist-mediated EMT pathways and could represent a promising therapeutic target for OSCC.

Clinical impact of the study

The identification of piR-35462 as a pivotal regulator of OSCC progression through the FTO/Twist1 axis presents a promising therapeutic target. Its role in promoting EMT and metastasis highlights the potential of targeting piR-35462 or its downstream effectors as a novel strategy for OSCC treatment. Furthermore, the detection of piR-35462 in exosomes suggests its potential as a non-invasive biomarker for early diagnosis, prognosis prediction and treatment monitoring in OSCC patients.

Putting in perspective

The discovery of piR-35462 as a mediator of EMT via FTO-dependent m6A demethylation provides new insights into the molecular mechanisms driving OSCC invasion and metastasis. Future research should focus on validating these findings in larger patient cohorts and exploring targeted therapeutic approaches that disrupt the piR-35462/FTO/Twist1 axis. Given the growing interest in RNA-based therapies, piR-35462 emerges as a promising target for the development of novel treatment strategies aimed at reducing OSCC aggressiveness and enhancing patient outcomes.

Abbreviations

CAFs	Cancer-associated fibroblasts
OSCC	Oral squamous cell carcinoma
NFs	Normal fibroblasts
FTO	Fat mass and obesity-associated protein
m6A	N6-methyladenosine
EMT	Epithelial-mesenchymal transition
piRNAs	PIWI-interacting RNAs
ATCC	American Type Culture Collection
GSEA	Gene Set Enrichment Analysis
CCK-8	Cell Counting Kit-8
α-SMA	α-smooth muscle actin
FAP	Fibroblast activation protein
CM	Onditioned mediums
TME	Tumor microenvironment
APC	Adenomatous polyposis coli
NES	Normalized enrichment score
FDR	False discovery rate

Supplementary Information

The online version contains supplementary material available at https://doi.org/10.1186/s12903-025-06082-3.

Supplementary Material 1

Supplementary Material 2

Supplementary Material 3

Supplementary Material 4

Acknowledgements

Not applicable.

Author contributions
SX designed and supervised the study, conducted the experiments, analyzed the data, and wrote the manuscript. SC and JL designed the study, analyzed the data, and revised the manuscript. YY, FW and BL conducted the experiments and analyzed the data. HM, LM, YP, XF, XT, MF, YT, TL, RW and SR conducted experiments and provided reagents. All authors have reviewed the manuscript.

Funding
This work was supported by Science and Technology Program of Guangzhou (Grant No. 202102010144); the National Natural Science Foundation of China (Grant No. 82272788); Guangdong Science and Technology Department (Grant No. 2024A1515012876); General Project of Guangzhou Basic and Applied Basic Research Project (2023A04J2110); CSCO-Meck Cancer Research Fund (Y-MSDZD2022-0459).

Data availability
All data utilized and/or analyzed in the current study are accessible from the corresponding author upon reasonable request.

Declarations

Ethics approval and consent to participate
This study has been approved by the ethics committee of Sun Yat-Sen Memorial Hospital, Sun Yat-Sen University (Approval Number: SYSKY-2024-014-01). Informed consent was obtained from all subjects prior to their participation in the research. All methods were conducted in accordance with relevant guidelines and regulations.

Patient consent for publication
Not applicable.

Competing interests
The authors declare no competing interests.

Author details
[1]Guangdong Provincial Key Laboratory of Malignant Tumor Epigenetics and Gene Regulation, Sun Yat-sen Memorial Hospital, Sun Yat-sen University, Building 3, Phase 2, 3rd Floor, Spiral Road East, Bio Island, Huangpu District, Guangzhou City, Guangdong Province 510120, China
[2]Department of Oral & Maxillofacial Surgery, Sun Yat-sen Memorial Hospital, Sun Yat-sen University, No. 107 Yanjiang West Road, Yuexiu District, Guangzhou City, Guangdong Province 510120, China
[3]Department of Pathology, The First Affiliated Hospital, Sun Yat-sen University, No. 58 Zhongshan Second Road, Yuexiu District, Guangzhou City, Guangdong Province 510080, China
[4]Department of Stomatology, The First Affiliated Hospital, Medical College of Shantou University, No. 57, Changping Road, Shantou City, Guangdong Province 515064, China

Received: 22 February 2024 / Accepted: 29 April 2025
Published online: 28 May 2025

References

1. Xia C, Dong X, Li H, et al. Cancer statistics in China and united States, 2022: profiles, trends, and determinants. Chin Med J (Engl). 2022;135(5):584–90.
2. Han B, Zheng R, Zeng H, et al. Cancer incidence and mortality in China, 2022. Journal of the National Cancer Center; 2024.
3. Sung H, Ferlay J, Siegel RL, et al. Global Cancer statistics 2020: GLOBOCAN estimates of incidence and mortality worldwide for 36 cancers in 185 Countries. CA Cancer J Clin. 2021;71(3):209–49.
4. Bilotta MT, Antignani A, Fitzgerald DJ. Managing the TME to improve the efficacy of cancer therapy. Front Immunol. 2022;13:954992.
5. Quail DF, Joyce JA. Microenvironmental regulation of tumor progression and metastasis. Nat Med. 2013;19(11):1423–37.
6. Peng C, Xu Y, Wu J, et al. TME-Related biomimetic strategies against Cancer. Int J Nanomed. 2024;19:109–35.
7. Yamamoto Y, Kasashima H, Fukui Y, et al. The heterogeneity of cancer-associated fibroblast subpopulations: their origins, biomarkers, and roles in the tumor microenvironment. Cancer Sci. 2023;114(1):16–24.
8. Fiori ME, Di Franco S, Villanova L, et al. Cancer-associated fibroblasts as abettors of tumor progression at the crossroads of EMT and therapy resistance. Mol Cancer. 2019;18(1):70.
9. Bremnes RM, Dønnem T, Al-Saad S, et al. The role of tumor stroma in cancer progression and prognosis: emphasis on carcinoma-associated fibroblasts and non-small cell lung cancer. J Thorac Oncol. 2011;6(1):209–17.
10. Song M, He J, Pan QZ, et al. Cancer-Associated Fibroblast-Mediated cellular crosstalk supports hepatocellular carcinoma Progression. Hepatology. 2021;73(5):1717–35.
11. Caligiuri G, Tuveson DA. Activated fibroblasts in cancer: perspectives and challenges. Cancer Cell. 2023;41(3):434–49.
12. Li Z, Sun C, Qin Z. Metabolic reprogramming of cancer-associated fibroblasts and its effect on cancer cell reprogramming. Theranostics. 2021;11(17):8322–36.
13. Bedeschi M, Marino N, Cavassi E et al. Cancer-Associated fibroblast: role in prostate Cancer progression to metastatic disease and therapeutic Resistance. Cells. 2023;12(5).
14. Chen B, Sang Y, Song X, et al. Exosomal miR-500a-5p derived from cancer-associated fibroblasts promotes breast cancer cell proliferation and metastasis through targeting USP28. Theranostics. 2021;11(8):3932–47.
15. Ren J, Ding L, Zhang D, et al. Carcinoma-associated fibroblasts promote the stemness and chemoresistance of colorectal cancer by transferring Exosomal LncRNA H19. Theranostics. 2018;8(14):3932–48.
16. Shi L, Zhu W, Huang Y, et al. Cancer-associated fibroblast-derived Exosomal microRNA-20a suppresses the PTEN/PI3K-AKT pathway to promote the progression and chemoresistance of non-small cell lung cancer. Clin Transl Med. 2022;12(7):e989.
17. Peng Z, Tong Z, Ren Z, et al. Cancer-associated fibroblasts and its derived exosomes: a new perspective for reshaping the tumor microenvironment. Mol Med. 2023;29(1):66.
18. Li C, Teixeira AF, Zhu HJ, et al. Cancer associated-fibroblast-derived exosomes in cancer progression. Mol Cancer. 2021;20(1):154.
19. Liu Y, Dou M, Song X, et al. The emerging role of the PiRNA/piwi complex in cancer. Mol Cancer. 2019;18(1):123.
20. Wang X, Ramat A, Simonelig M, et al. Emerging roles and functional mechanisms of PIWI-interacting RNAs. Nat Rev Mol Cell Biol. 2023;24(2):123–41.
21. Xie Q, Li Z, Luo X, et al. piRNA-14633 promotes cervical cancer cell malignancy in a METTL14-dependent m6A RNA methylation manner. J Transl Med. 2022;20(1):51.
22. Wu D, Fu H, Zhou H, et al. Effects of novel NcRNA molecules, p15-piRNAs, on the methylation of DNA and histone H3 of the CDKN2B promoter region in U937 Cells. J Cell Biochem. 2015;116(12):2744–54.
23. Zhang L, Meng X, Pan C, et al. PiR-31470 epigenetically suppresses the expression of glutathione S-transferase pi 1 in prostate cancer via DNA methylation. Cell Signal. 2020;67:109501.
24. Han H, Fan G, Song S, et al. piRNA-30473 contributes to tumorigenesis and poor prognosis by regulating m6A RNA methylation in DLBCL. Blood. 2021;137(12):1603–14.
25. Ding X, Li Y, Lü J, et al. piRNA-823 is involved in Cancer stem cell regulation through altering DNA methylation in association with luminal breast Cancer. Front Cell Dev Biol. 2021;9:641052.
26. Shi S, Yang ZZ, Liu S, et al. PIWIL1 promotes gastric cancer via a piRNA-independent mechanism. Proc Natl Acad Sci U S A. 2020;117(36):22390–401.
27. Zhao S, Gou LT, Zhang M, et al. piRNA-triggered MIWI ubiquitination and removal by APC/C in late spermatogenesis. Dev Cell. 2013;24(1):13–25.
28. Amaar YG, Reeves ME. The impact of the RASSF1C and PIWIL1 on DNA methylation: the identification of GMIP as a tumor suppressor. Oncotarget. 2020;11(45):4082–92.
29. Li B, Xie S, Pan G, et al. Circ-OMAC drives metastasis in oral squamous cell carcinoma. Oral Dis; 2022.
30. Li Y, Tao Y, Gao S, et al. Cancer-associated fibroblasts contribute to oral cancer cells proliferation and metastasis via exosome-mediated paracrine miR-34a-5p. EBioMedicine. 2018;36:209–20.
31. Wang N, Li X, Zhong Z, et al. 3D hESC exosomes enriched with miR-6766-3p ameliorates liver fibrosis by attenuating activated stellate cells through targeting the TGβRII-SMADS pathway. J Nanobiotechnol. 2021;19(1):437.
32. Abu EO, Horner A, Teti A, et al. The localization of thyroid hormone receptor mRNAs in human bone. Thyroid. 2000;10(4):287–93.

33. Xie SL, Fan S, Zhang SY, et al. SOX8 regulates cancer stem-like properties and cisplatin-induced EMT in tongue squamous cell carcinoma by acting on the Wnt/β-catenin pathway. Int J Cancer. 2018;142(6):1252–65.
34. Su J, Li Y, Liu Q, et al. Identification of SSBP1 as a ferroptosis-related biomarker of glioblastoma based on a novel mitochondria-related gene risk model and in vitro experiments. J Transl Med. 2022;20(1):440.
35. Peng Y, Xiong RP, Zhang ZH, et al. Ski promotes proliferation and inhibits apoptosis in fibroblasts under high-glucose conditions via the FoxO1 pathway. Cell Prolif. 2021;54(2):e12971.
36. Zhao Y, He M, Cui L, et al. Chemotherapy exacerbates ovarian cancer cell migration and cancer stem cell-like characteristics through GLI1. Br J Cancer. 2020;122(11):1638–48.
37. Symons RA, Colella F, Collins FL, et al. Targeting the IL-6-Yap-Snail signalling axis in synovial fibroblasts ameliorates inflammatory arthritis. Ann Rheum Dis. 2022;81(2):214–24.
38. Yue J, Wang P, Hong Q, et al. MicroRNA-335-5p plays dual roles in periapical lesions by complex regulation Pathways. J Endod. 2017;43(8):1323–8.
39. Yang E, Wang X, Gong Z, et al. Exosome-mediated metabolic reprogramming: the emerging role in tumor microenvironment remodeling and its influence on cancer progression. Signal Transduct Target Ther. 2020;5(1):242.
40. Li C, Ni YQ, Xu H, et al. Roles and mechanisms of Exosomal non-coding RNAs in human health and diseases. Signal Transduct Target Ther. 2021;6(1):383.
41. Ou B, Liu Y, Gao Z, et al. Senescent neutrophils-derived Exosomal piRNA-17560 promotes chemoresistance and EMT of breast cancer via FTO-mediated m6A demethylation. Cell Death Dis. 2022;13(10):905.
42. Howard A, Agrawal N, Gooi Z. Lip and oral cavity squamous cell Carcinoma. Hematol Oncol Clin North Am. 2021;35(5):895–911.
43. Chen Y, McAndrews KM, Kalluri R. Clinical and therapeutic relevance of cancer-associated fibroblasts. Nat Rev Clin Oncol. 2021;18(12):792–804.
44. Wen S, Hou Y, Fu L, et al. Cancer-associated fibroblast (CAF)-derived IL32 promotes breast cancer cell invasion and metastasis via integrin β3-p38 MAPK signalling. Cancer Lett. 2019;442:320–32.
45. Liang T, Tao T, Wu K, et al. Cancer-Associated Fibroblast-Induced remodeling of tumor microenvironment in recurrent bladder Cancer. Adv Sci (Weinh). 2023;10(31):e2303230.
46. Ma C, Yang C, Peng A, et al. Pan-cancer spatially resolved single-cell analysis reveals the crosstalk between cancer-associated fibroblasts and tumor microenvironment. Mol Cancer. 2023;22(1):170.
47. Wang D, Wang X, Song Y, et al. Exosomal miR-146a-5p and miR-155-5p promote CXCL12/CXCR7-induced metastasis of colorectal cancer by crosstalk with cancer-associated fibroblasts. Cell Death Dis. 2022;13(4):380.
48. Zheng S, Tian Q, Yuan Y, et al. Extracellular vesicle-packaged circBIRC6 from cancer-associated fibroblasts induce platinum resistance via sumoylation modulation in pancreatic cancer. J Exp Clin Cancer Res. 2023;42(1):324.
49. Zhuang J, Shen L, Li M, et al. Cancer-Associated Fibroblast-Derived miR-146a-5p generates a niche that promotes bladder Cancer stemness and Chemoresistance. Cancer Res. 2023;83(10):1611–27.
50. Pakravan K, Mossahebi-Mohammadi M, Ghazimoradi MH, et al. Monocytes educated by cancer-associated fibroblasts secrete Exosomal miR-181a to activate AKT signaling in breast cancer cells. J Transl Med. 2022;20(1):559.
51. Zhou J, Xie H, Liu J, et al. PIWI-interacting RNAs: critical roles and therapeutic targets in cancer. Cancer Lett. 2023;562:216189.
52. Zhang Q, Zhu Y, Cao X, et al. The epigenetic regulatory mechanism of PIWI/piRNAs in human cancers. Mol Cancer. 2023;22(1):45.
53. Shen S, Yu H, Liu X, et al. PIWIL1/piRNA-DQ593109 regulates the permeability of the Blood-Tumor barrier via the MEG3/miR-330-5p/RUNX3 Axis. Mol Ther Nucleic Acids. 2018;10:412–25.

Publisher's note